Investigating the Advantages of Magnetomyography in Assistive Healthcare Technology

Negin Ghahremani Arekhloo[1,2], Hossein Parvizi[1], Siming Zuo[1,2], Huxi Wang[1,2], Kianoush Nazarpour[2,3] and Hadi Heidari[1,2]
[1]James Watt School of Engineering, University of Glasgow, G12 8QQ, UK
[2]Neuranics Ltd., Glasgow, United Kingdom
[3]School of Informatics, The University of Edinburgh, EH8 9AB, UK
hadi.heidari@glasgow.ac.uk

***Abstract*—Assistive healthcare technologies and prosthetics are crucial for individuals with muscle impairments. In 2005, the number of limb losses from trauma exceeded 700,000, projected to double by 2050, affecting approximately 1,326,000 civilians. Understanding the fundamental principles of muscle function, therefore, is key to developing innovative assistive technologies that can improve the quality of life for people with disabilities. Surface electromyography (sEMG), measuring electrical muscle activity, has long been a common tool in assistive technologies, but various obstacles have limited its widespread application. Capturing sEMG signals via the skin and subcutaneous fat poses a main challenge as they act as a low-pass filter and lead to the loss of critical information. Thus, new alternative technologies are needed to address this challenge. Magnetomyography (MMG) is a technology that can noninvasively measure magnetic muscle signals. Unlike sEMG, MMG signals are not affected by various tissues as they are transparent for magnetic signals. This paper presents the fundamental scenarios, including fat thickness on the EMG and MMG signals, with finite element (FE) simulations using COMSOL. The effects of 50-750 µm fat on the recorded electrical and magnetic signals have been evaluated. The results indicate that by increasing fat thickness to 250 µm, the electrical signals decrease 66%, while MMG signals decline by 12%. Hence, the MMG can provide more accurate measurements of muscle activity for control strategies in prosthetic limbs.**

Keywords—Assistive Healthcare Technology, Electrical signal, Electromyography, EMG, Fat effect, MMG, Magnetic signal, Magnetomyography, Prosthetics

I. INTRODUCTION

Assistive healthcare technology covers a wide range of tools, software, and services designed to empower individuals with disabilities and age-related limitations to lead more independent lives [1]. Among these technologies, prosthetic limbs are crucial in restoring functional mobility and independence in individuals with limb loss (amputation). In 2005, the number of amputations from trauma exceeded 700,000, projected to double by 2050, affecting approximately 1,326,000 civilians [2]. In response to this growing need, prosthetic technology has progressed significantly, offering a range of options regarding cosmetic designs and levels of functionality [3]. To improve functionality, prosthetic limbs are equipped with diverse control systems and strategies to empower users in effectively manipulating and controlling their artificial limbs. One commonly used control system relies on surface electromyography (EMG), which is based on the electrical signals generated in the skeletal muscle and reflects users' intentions. As shown in Fig.1A, when a user intends to perform a specific movement, like grasping a cup

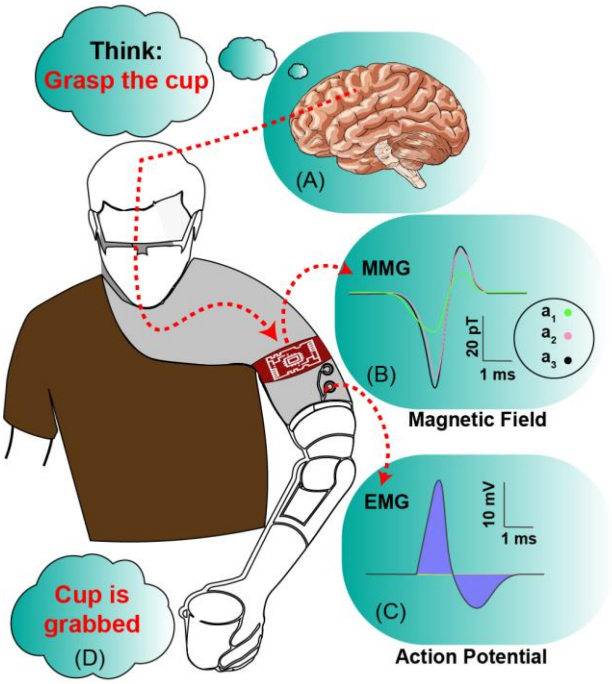

Fig. 1: Control technologies in prosthetic limbs. (A) User intention in the brain and the signals travelling to the target muscles (B) MMG signals. (C) EMG signals. (D) The intention is completed.

with their prosthetic hand, the corresponding muscles involved in that action generate specific patterns of electrical activity. The EMG sensors (Fig.1C) on the skin overlying the target muscles can capture and analyse these patterns. By detecting and analysing these electrical signals, prosthetic control systems can interpret the user's intention and translate it into the desired action of the prosthetic limb, as shown in Fig. 1D).

Despite the extensive use of EMG signals in prosthetic control since 1948 [4], precisely decoding and utilising EMG signals for device control remains challenging. These difficulties stem from several factors, including the influence of various layers between the signal source and skin surface, including muscle, fat, and connective tissue, on the recorded signals, with fat having a particularly significant impact. Additionally, changes in electrode position, sweat at the electrode site, alterations in the impedance of the electrode-skin contact, and interelectrode distance can further modify the signals [5]. These limitations led to the development of Magnetomyography (MMG), a technique introduced by Cohen and Gilver in 1972 [6], which enables the measurement of muscle activity via magnetic fields, as depicted in Fig.1B. This technique exploits the physiological phenomenon of electrical activity occurring within the human muscle, serving as a source of the biomagnetic signal. Unlike electrical signals, the human body's permeability to magnetic fields remains constant and is minimally affected by the inhomogeneous conductivity of body tissue, making them more reliable for detecting biological phenomena [7]. Moreover, MMG does not require direct contact between the skin and the sensor for detecting magnetic signals. As a result, challenges associated with changes in skin and electrode impedance, sweat on the skin, and interelectrode distance are eliminated in MMG. This non-contact detection method greatly enhances the feasibility and accuracy of capturing magnetic muscle signals. The evolution of electric and magnetic field is explained by Maxwell's equations. Using the quasi-static electrical field equations as a starting point, we incorporate appropriate modelling assumptions within a finite element (FE) analysis platform. This enables us to simulate the electro-physiological behaviour of skeletal muscle under various subcutaneous fat thickness, allowing a comparison between recorded EMG and MMG signals.

II. Methodology

As the timescale for magnetic and electrical field changes are very slow, differentiated forms of Maxwell's equation are:

$$\nabla.\boldsymbol{E} = \frac{\boldsymbol{\rho}}{\boldsymbol{\varepsilon_0}} \qquad \nabla \times \boldsymbol{E} = 0 \qquad \nabla.\mathbf{j} = 0 \tag{1}$$

Therein, $\mathbf{E}$ is the electrical field, $\boldsymbol{\rho}$ is the electrical charge density, $\boldsymbol{\varepsilon_0}$ is vacuum electrical permittivity, $\mathbf{j}$ is electric current density vector. Electrical scalar potential within our Finite Element (V_{FE}) model is described by equation (2), which is derived from Ampere's law. It considers both conductivity (σ) and permittivity ($\varepsilon = \varepsilon_0\varepsilon_r$), therein ε_r is the relative permittivity of the tissue. [8].

$$-\nabla.([\sigma]\nabla V_{FE}) - \nabla([\varepsilon]\nabla\frac{\partial V_{FE}}{\partial t}) = 0 \tag{2}$$

Due to the anisotropic nature of muscle fibres, where electrical properties vary significantly along the axial and radial directions, it is crucial to consider these directional variations. While the literature offers a wide range of values for σ and ε in each layer, we have specifically employed tissue parameters for our FE simulation, which are listed in Table 1.

Table 1: Tissue electrical and magnetic parameters

Material	Electrical Conductivity (σ)	Relative Permittivity (ε)	Relative Permeability
Skin	0.0003	6000	1
Fat	0.0303	25000	1
CT	0.49	5.39e5	1
EF	0.04	1.31e6	1
MF (Radial)	0.027	5.2e5	1
MF (Axial)	0.08	1.31e6	1
Electrode	0.003	1	1

CT: Connective Tissue; **EF**: Extracellular Fluid; **MF**: Muscle Fiber

A. Modelling Framework

Our model is designed to provide a comprehensive representation of the various components of the human body. These components include muscle fibers, extracellular fluid, connective tissue, fat, and skin, as shown in Fig.2B in a 3D structure. To capture the two-dimensional characteristics of these elements, we organized them in a rectangle structure, with each component having a different thickness: muscle fiber (40 µm), extracellular fluid (10 µm), connective tissue (20 µm), fat (50-750 µm), and skin (100 µm), as depicted in Fig.3A. To stimulate the muscle fibers, we place a pair of electrodes, with 0.005 mm inter-electrode distance, on the surface of the skin, as illustrated in Fig. 2A and 3B. The stimulation input current follows an asymmetrical biphasic pattern and is defined as $I_0 \times g(t)$, where I_0 is the initial constant current of 10 mA, and g(t) is the step time function, as shown in Fig.3C.

In terms of the boundary condition, the absence of current within the structure results in a Neumann boundary condition of zero. This means there is no electrical charge flow or movement across the boundary. Additionally, the electrical potential remains consistent at the interface between different components. Finally, considering a ground electrode in our model (structure), we also account for the Dirichlet boundary condition.

As the computationally challenging nature of simulating the entire body, the domain of interest is typically confined to a representative region comprising a single muscle fiber, extracellular fluid, connective tissue, subcutaneous fat, and skin. This restricted domain allows for more manageable computational analysis while still capturing the essential components relevant to the study.

B. Electric and Magnetic Response

In our study, we initially examined the response of the single muscle to the biphasic stimulation over the skin surface. To achieve this, we selected two points within the muscle fiber, shown in Fig.3A, spaced 0.1 mm apart, and measured the potential difference between them, known as a muscle action potential, which is shown in Fig.3D. To enhance the clarity of the observed changes between these two points in the muscle fiber, we also analyzed the single derivative of the muscle response, as depicted in Fig.3B.

Additionally, we conducted an analysis of the electro-magnetic characteristics by examining both the "Electrical Field Norm" and "Magnetic Flux Density" using surface plots.

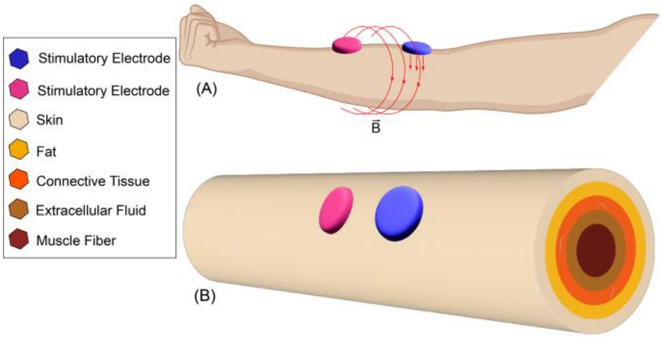

Fig.2: (A) Inward current stimulates the forearm muscle causing a magnetic field around the muscle; (B) 3D view of the structure representative of various components of the human body and the stimulatory electrodes.

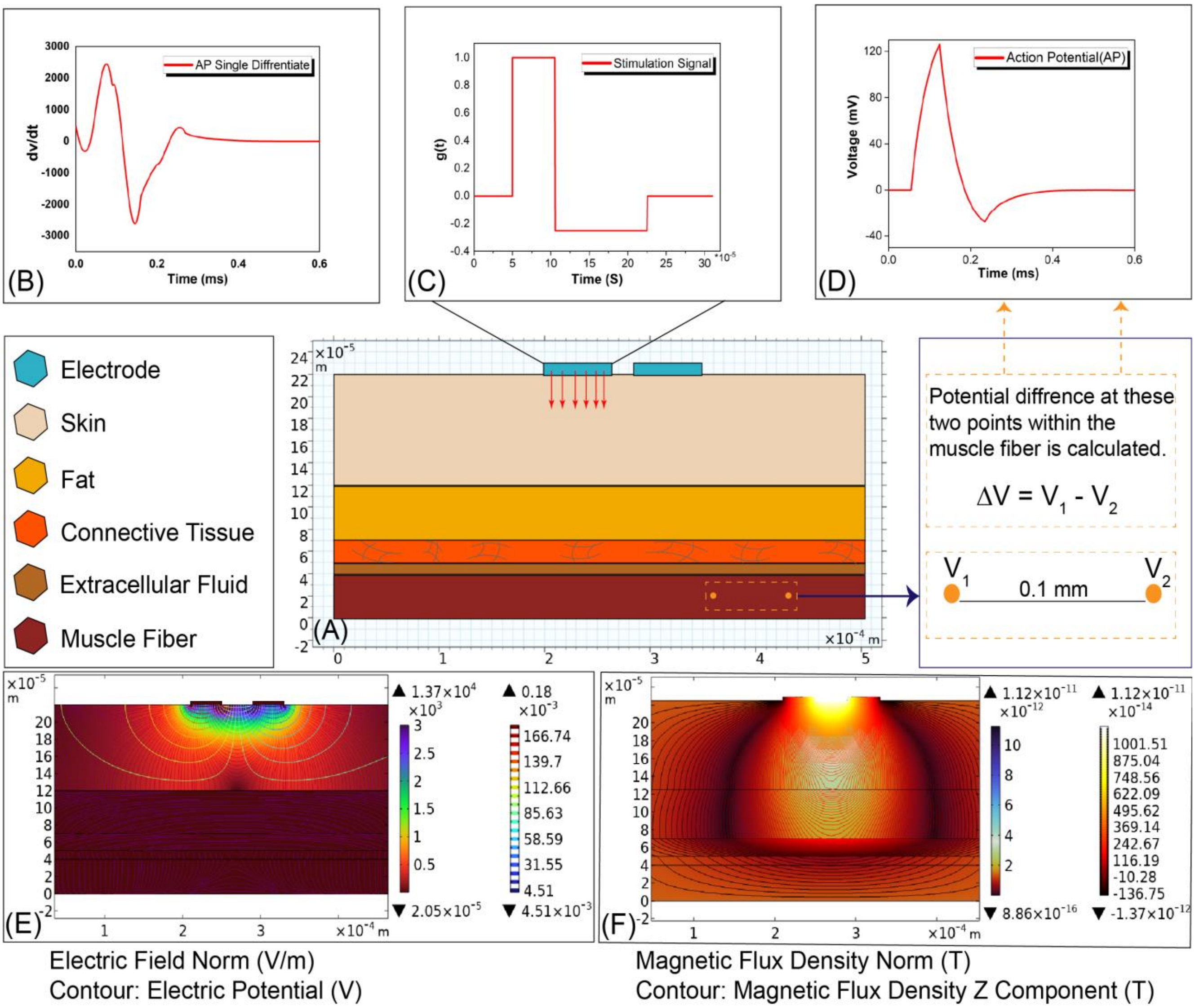

Fig.3: Electromagnetic characteristics. (A). Model structure illustration. (B) Single derivative of action Potential. (C) The biphasic shape of a stimulatory signal from the electrode. (D). Action Potential is calculated by measuring the potential difference between two points inside the muscle fiber. E) Surface plot and the contour line of the Electric Field Norm. F) Surface plot and the contour line of the Magnetic Flux Density Norm.

The "Electrical Field Norm" provided valuable insights into the intensity and distribution of the electric field within our model, representing the magnitude or strength of the electric field vector at each point on the surface of interest. Similarly, through surface plots, we examined the "Magnetic Flux Density", which quantifies the strength or intensity of the magnetic field at specific points. It is worth mentioning that we could only record the Z component of the magnetic signal, which is perpendicular to our current. This comprehensive analysis allowed us to determine the strength and distribution of electric and magnetic field vectors at each point in the surface in response to the applied biphasic stimulating signal. The surface plots included contour lines, which visually represent the field distribution and their potential effects on the surrounding structure.

Interestingly, the surface plot analysis revealed that the magnetic field remained undistorted as it passed through different tissue layers, in contrast to the electrical field, as depicted in Fig.3E and 3F. This outcome aligns with our expectations [9], as all tissues possess a relative permeability of 1, indicating minimal influence on magnetic field property.

C. Fat Effect

To assess the impact of varying fat thickness on electric and magnetic signals, we conducted recordings within muscle fibers featuring different fat thicknesses Our range spanned from 50 µm to 750 µm, with increments of 50 µm. Throughout the simulation, a consistent electrical stimulation intensity was maintained. As depicted in Fig.4, we observed a significant decline of 66% in the electrical signals beyond the 250 µm mark. Subsequently, at the 400 µm point, the signals became exceedingly weak. Conversely, magnetic signals exhibited a decrease of only 12.5% after the 250 µm threshold, aligning with findings reported in existing literature [10, 11].

III. Results and Discussion

This work is implemented to show the subcutaneous fat thickness on the electric and magnetic signal. To achieve this, we conducted simulations using the finite element platform, specifically COMSOL. Initially, we evaluated the electric and magnetic effects in surrounding tissues after applying electrical stimulation to the skin surface overlying the muscle fibers. By utilizing biphasic stimulation on the skin surface,

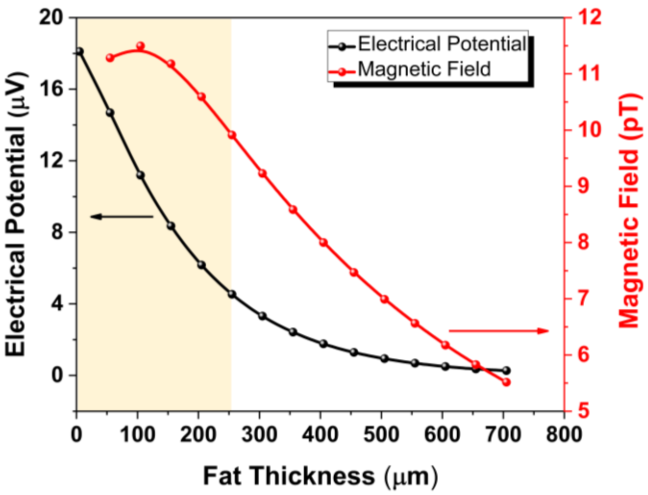

Fig 4. The effect of fat thickness on the magnetic and electric signals. After 250 µm, there is a 66% decline in the electrical signals, but there is a 12% decline in the magnetic field.

we recorded the muscle action potential within the muscle. To enhance the clarity of potential changes, we applied the single derivative of the action potential in response to the stimulating signals. Then, the electric field norm and magnetic flux density surface plots are employed to illustrate the representation of electric and magnetic signals. The plots demonstrated that the electric signals experience while traversing the diverse layers between the skin and muscle fiber. In contrast, the magnetic signals remain unaffected as they pass through these different layers. Furthermore, in order to assess the impact of subcutaneous fat thickness, a critical layer, on the measured magnetic and electrical signals, we conducted an evaluation across a range of fat thicknesses from 50 to 750 µm. The results, as demonstrated in Fig.4, highlight a notable pattern. After reaching approximately 250-300 µm of fat thickness, there is a significant decrease, about 66%, observed in the electrical signals, rendering them considerably weaker. This decline can be attributed to the attenuation caused by the intervening layers, acting as a low-pass filter, which is in agreement with the literature [12].

Conversely, the magnetic signals exhibit a less pronounced decrease, with only a 12% reduction. This suggests that due to the relative permeability of the layers between the muscle and skin, which remains constant at one, recorded magnetic signals are minimally affected. The observed decline in magnetic signals can likely be attributed to the increasing distance between the signal source and the sensor, rather than the tissues acting as a low-pass filter for the magnetic signals.

These findings highlight the significance of subcutaneous fat thickness in affecting the strength of electrical signals. The electric field experiences more substantial attenuation compared to the magnetic field, which remains relatively unaffected. Understanding the variations in signal strength and integrity due to different tissue layers is critical for the accurate interpretation and analysis of muscle signals. This knowledge plays a vital role in developing effective control strategies for prosthetic hand control. By accurately interpreting the electrical and magnetic signals as they pass through different layers, researchers can refine control algorithms to precisely capture and translate the user's intended movements into actions performed by the prosthetic hands.

IV. Conclusion and Future Work

Improved understanding of signal behaviour enables more accurate and intuitive control, enhancing the overall functionality and usability of prosthetic hands. So, in this paper, first of all, we evaluate the effect of magnetic and electrical field in surrounding tissues following the electrical stimulation over the human skin. However, the electrical field experienced a notable decline, with a 66% decrease observed when stimulating muscles with varying subcutaneous fat thicknesses ranging from 50 to 750 µm. Conversely, the decline in magnetic signals was only 12%. So, the tissues act as a low-pass filter for electrical signals, while remaining transparent to the magnetic signals. Regarding the future work, our research will primarily focus on investigating the effects of other fundamental factors, such as muscle fiber depth, on the behaviours of MMG and EMG signals. By expanding our understanding of these scenarios, we can further refine and optimize prosthetic control strategies to enhance functionality and precision of prosthetic hands.

Acknowledgement

The research leading to these results received funding from the Scottish Research Partnership in Engineering - SRPe (PEER1718/03). This work was partially supported by EPSRC IAA projects EP/X5257161/1. The authors are also thankful to the University of Glasgow for funding received under the Glasgow Exchange Knowledge (GKE) Fund 2017/2018.

References

[1] G. E. Lancioni, N. N. Singh, M. F. O'Reilly, J. Sigafoos, and D. Oliva, "Assistive technology for people with severe/profound intellectual and multiple disabilities," *Assistive technologies for people with diverse abilities*, pp. 277-313, 2014.

[2] K. Ziegler-Graham, E. J. MacKenzie, P. L. Ephraim, T. G. Travison, and R. Brookmeyer, "Estimating the prevalence of limb loss in the United States: 2005 to 2050," *Archives of physical medicine and rehabilitation*, vol. 89, no. 3, pp. 422-429, 2008.

[3] P. Geethanjali, "Myoelectric control of prosthetic hands: state-of-the-art review," *Medical Devices: Evidence and Research*, pp. 247-255, 2016.

[4] R. Reiter, "Eine neue elektrokunsthand," *Grenzgebiete der Medizin*, vol. 1, no. 4, pp. 133-135, 1948.

[5] P. Artemiadis, "EMG-based robot control interfaces: past, present and future," *Advances in Robotics & Automation*, vol. 1, no. 2, pp. 1-3, 2012.

[6] D. Cohen and E. Givler, "Magnetomyography: Magnetic fields around the human body produced by skeletal muscles," *Applied Physics Letters*, vol. 21, no. 3, pp. 114-116, 1972.

[7] H. Wang, *et al.*, "Wearable super-resolution muscle–machine interfacing," *Frontiers in Neuroscience*, vol. 16, p. 1020546, 2022.

[8] A. Kuhn, *et al.*, "A model for transcutaneous current stimulation: simulations and experiments," *Medical & biological engineering & computing*, vol. 47, pp. 279-289, 2009.

[9] N. Ghahremani Arekhloo *et al.*, "Alignment of magnetic sensing and clinical magnetomyography," *Frontiers in Neuroscience*, vol. 17, p. 1154572, 2023.

[10] N. G. Arekhloo *et al.*, "Investigating the Volume Conduction Effect in MMG and EMG during Action Potential Recording," in *2022 29th IEEE International Conference on Electronics, Circuits and Systems (ICECS)*, 2022: IEEE, pp. 1-4.

[11] T. Klotz, L. Gizzi, and O. Röhrle, "Investigating the spatial resolution of EMG and MMG based on a systemic multi-scale model," *Biomechanics and Modeling in Mechanobiology*, vol. 21, no. 3, pp. 983-997, 2022.

[12] S. Zuo, H. Heidari, D. Farina, and K. Nazarpour, "Miniaturized magnetic sensors for implantable magnetomyography," *Advanced Materials Technologies*, vol. 5, no. 6, p. 2000185, 2020.